SERS-Active Gold Lace Nanoshells with Built-in Hotspots

ARTICLE *in* NANO LETTERS · OCTOBER 2010

Impact Factor: 13.59 · DOI: 10.1021/nl101946c · Source: PubMed

Published in final edited form as:
Nano Lett. 2010 October 13; 10(10): 4013–4019. doi:10.1021/nl101946c.

SERS-Active Gold Lace Nanoshells with Built-in Hotspots

Ming Yang[1], **Ramón Alvarez-Puebla**[4], **Hyoung-Sug Kim**[#], **Paula Aldeanueva-Potel**[4], **Luis M. Liz-Marzán**[*,4], and **Nicholas A. Kotov**[*,1,2,3,4]

[1]Department of Chemical Engineering, University of Michigan, Ann Arbor, MI 48109

[#]R&D Center, Hepce Chem Co., Ltd., Ansan, Kyounggi-Do, South Korea, 425–836

[2]Department of Material Sciences and Engineering, University of Michigan, Ann Arbor, MI 48109

[3]Departments of Biomedical Engineering, University of Michigan, Ann Arbor, MI 48109

[4]Departamento de Química Física and Unidad Asociada CSIC, Universidade de Vigo, 36310 Vigo, Spain

Abstract

Development of multifunctional drug delivery vehicles with therapeutic and imaging capabilities as well as *in-situ* methods of monitoring of intracellular processes will greatly benefit from a simple method of preparation of plasmonic Au structures with nanometer scale gaps between sharp metallic elements where the so called SERS hot spots can be formed. Here the synthesis of gold lace capsules with average diameters ca. 100 nm made of a network of metallic branches 3–5 nm wide and separated by 1–3 nm gaps is reported. Biocompatible amphiphilic polyurethanes (PUs) were used as template for these particles. The unusual topology of the produced gold lace shells somewhat reminiscent of Fabergé eggs is likely to reflect the network of hydrophobic and hydrophilic domains of PU globules. The gold lace develops from initial open web-like structures by gradual enveloping the PU template. The diameter of gold lace shell is determined by the size of PUs in water and can be adjusted by the molecular mass of PUs. The close proximity between branches makes them excellent supports for surface enhanced Raman spectroscopy (SERS) which was demonstrated using 1-naphthalenethiol upon excitation with photons with different wavelengths. The loading and releasing of pyrene as a model of hydrophobic drugs and the use of SERS to monitor it were demonstrated.

Keywords

plasmonic shells; theranostic; polyurethane; Au nanoparticles; template; drug delivery; SERS; hotspots

INTRODUCTION

High mobility of electrons in nanoparticles (NPs) of noble metals1a–d leads to unusually high absorption cross sections and plasmon resonances in UV-vis-NIR range, which makes them uniquely suitable for a variety of applications.1e–h Similarly to semiconductor NPs, the optical properties of metallic NPs are strongly shape- and size-dependent,2 which can be exemplified by NPs shaped as cubes,1b rods2 and wires,3a plates3b,c cages3d prisms,3e stars,5c *etc*. For Au NPs4 these properties are combined with nearly negligible toxicity to mammalian cells, which has spurred multiple biomedical studies including both the

lmarzan@uvigo.es, kotov@umich.edu.

treatment of cancer4e by photoinduced hyperthermia4j,m and its diagnostics by photoacoustic imaging4f,i or SERS.4p Both spherical and intricately shaped Au NPs can also be used for drug delivery benefiting from simple bioconjugation to Au surface via –SH bonds.4g,k In many ways, Au NPs represent an ideal materials platform for theranostics - a rapidly evolving subset of medical techniques allowing real-time observation of the tissue during treatment and intra-organ distribution of the treatment agent or drug carrier. Development of SERS capabilities for each individual particle makes also possible multiple applications for *in-situ* monitoring of biological processes including drug release or the physiological changes inside the cells in real time.

However, the nanoscale and molecular structure of NPs made so far may not be optimal for these multiple tasks and, in particularly, for SERS. In respect to the drug delivery function(s), the mode of drug transport as a two-dimensional (2D) monolayer adsorbed to Au surface is not the best because of reduced capacity compared to storage in three-dimensional (3D) space and limitations on the drug chemistry (*e.g.* presence of –SH groups). Ideally, such agents would have a structure of a rod or shell with near IR adsorption1g and an accessible polymeric compartment inside it for drug loading. While the use of thermosensitive polymer-covered gold cages4n and liposome-gold nanocontainers4o as drug carriers had been suggested, there are still some key improvements to be made. It would be quite important to: have a better control over particle diameter to avoid fast capture by macrophages (when too big) and renal clearance (when too small) and to reduce the overall amount of Au in the agents as a non-biodegradable compound. Simplification of preparative methods for such engineered NPs1g, 4n, 4o will also be an added benefit.

For both therapeutic and diagnostic functions it will be quite essential to engineer pores and gaps in the Au coating with the range of dimensions of 1–10 nm. Their realization was definitely associated with considerable synthetic problems. At the same time, having gaps and pores in the plasmonic shells will make the inner volume more accessible and will make possible to control the release of the drugs by opening and closing them using established techniques4n. They will also form very convenient and hopefully multiple on-particle hotspots necessary for SERS. This will be exceptionally useful for the tasks of in-situ monitoring of cell processes with unprecedented resolution and label free.

In this paper we show that NPs with such structural characteristics, optical and synthetic properties are possible. Shell-like NPs composed of small Au “fingers” and nanoscale gaps between them resembling intricate network of gold lace can be made by using polyurethanes (PUs). To some degree they are reminiscent of Fabergé eggs in terms of the shape, topology, material, and function, but except the dimensions. The average diameter of such gold lace shells can be controlled by the molecular mass of PUs. The entrapped PUs inside gold shells can be used as drug carrier which is confirmed by the loading and releasing of molecules of pyrene serving as a model of hydrophobic small molecule drugs common in medical practice. Due to close plasmon coupling between branches, these structures act as excellent substrates for optical enhanced spectroscopies such as SERS. We demonstrate that, due to their particular structure, these particles induce a considerably larger enhancement than spherical particles of similar size, because they act as single particle hotspots in suspension. The high intensity of the SERS signal has allowed us to undoubtedly monitor the uptake and release of pyrene.

RESULTS AND DISCUSSION

This work was focused on utilizing waterborne PUs in preparation of Au NPs due to exceptional structural versatility of these polymers and unrivaled possibilities compared to most other polymers for tuning different physical, chemical, and biological properties. From

the point of view of NP synthesis, this translates into the ability to continuously vary morphology of the produced NPs leading hopefully to the desired shapes and functional properties. Also, enhanced biostability and biocompatibility have been demonstrated based on the blending some of PUs and NPs.6 In respect to biomedical applications PUs also have a number of advantages in respect to traditional surfactants. As well, they are one of the most bio-, blood-compatible materials known today and played a major role in the development of many medical devices ranging from catheters to the artificial heart.7

Synthesis of Au nanocolloids usually employs surfactants as structure-directing agents (for example, CTAB for nanorods,2 PVP for nanocubes,1b amine for nanowires3a), which coat the particles at water-metal interface. Even the intricate shapes of Au NPs for applications in SERS or nanoplasmonics,8 such as dendrites,5a multipods,5b nanostars,5c nanoflowers5d and shells5e *etc* were also made using different surfactants but the same general approach. Initially, it was expected that the waterborne PUs utilized here (Figure 1a) would act similarly, but they exhibit structural control over Au nanocolloids in a markedly different way.

Gold lace nanocapsules with average diameters ca. 100 nm were obtained by simple mixing a solution of PU-1 (Figure 1a, Mw=92 kDa, cationic site content 2.42%) with $HAuCl_4$ followed by reduction with ascorbic acid at room temperature. The reaction is exceptionally simple. SEM and TEM imaging indicates that the walls of these Au NPs are made of Au “fingers” 3–5 nm wide intricately interconnected in an intricate dentritic pattern derived from interdigitation of individual elongated branches with multiple open pores. The branches, or fingers are separated by the gaps of ca. 1–3 nm (Figure 1b–f). Open shells can also be found and confirm the hollow morphology (Figure 1e) of the particles. When the concentration of $AuCl_4^-$ is reduced, the complete gold shells gradually transform into gold dendrites or “octopuses” (Figure 2a–i) exacerbating the lace-like morphology. In this case the Au branches cannot grow over the entire PU spheres but cover a part of the surface of the PU globules providing a replica of domains existing on its surface.

The observed crystal lattice spacing of 0.289 nm matches that of Au (111) crystal planes (Figure 1f). Importantly, the diameter of the gold lace shells is matches very well the diameter of the PU-1 globules, MW ≈ 92 kDa, determined by AFM (Fig.1g). This conclusion is also confirmed by the measurements of the hydrodynamic diameter of the PU-1 by light scattering (Supplem. Mater. Fig. S1). PU globules have quasi sphere-like structures and a size distribution in water centered around 130 nm (Supplem. Mater. Fig.S1). The positive value of zeta potential (Supplem. Mater. Fig.S1) indicates that the hydrophilic amine groups (Figure 1a) reside on the surface of PU globules. Such micelle-like structures of water-soluble PU were also suggested in previous studies.9c–e Upon the addition of $AuCl_4^-$, ionic pairs $\{AuCl_4^- \bullet\bullet\bullet N^+\}$ should form serving as nucleation sites for reduction and crystallization of Au. It is likely that, due to the thermodynamic incompatibility of the hard segments (HS) and soft segments (SS) in PU, the polymer system is forced to form a localized two-phase morphology in which hydrophilic amine-rich hard domains are separated by hydrophobic soft domains.9 The HS carrying positive charges can form fibrillar microdomains through hydrogen bonding. 9b As a result, the growth of gold islands on the surface of PU spheres is not continuous but molded into the interconnected strands.

The waterborne PU acts as a template for Au NPs where the polymer directs the topology of the NP using different physical constrains than other polymers and surfactants used before. 1b,2,3a In comparison with them, PU globules are more robust and less prone to restructure around the NPs accommodating the growing gold core but rather forcing the NPs to grow around them. Potential thermodynamic benefits of covering the hydrophobic domains of PU with Au should also be considered.

Following this idea, one might expect that the topology of the gold lace shells can be controlled by the physical/geometrical parameters of PU globules. As such, using PU-2 with smaller molecular mass of *ca.* 77 kDa (cationic site content of 6%), smaller gold shells might be obtained. Indeed, the diameter of shells template by PU-2 is *ca.* 50 nm (Figure 2j–l) which is comparable hydrodynamic diameter of PU-2 of 70 nm (Figure S2a).

Generally, the branched structures gold lace shells show broad absorption spectra spanning the window from 480 nm to 1000 nm (Supplem. Mater. Fig. S2). The peak observed before 600 nm can be related to the transversal oscillations in the branches, while the IR tail for PU-1 templated Au shells (Supplem. Mater. Fig. S2) and the peak around 740 nm for PU-2 templated Au NPs (Supplem. Mater. Fig. S2) can be attributed to longitudinal plasmons distorted by coupling to adjacent branches generating highly active optical hotspots.10 It is interesting to note that the longitudinal plasmon band dominates the absorption spectra of PU-2 templated smaller shells. This observation correlates well with the average width of the branches for the two templates. It is more than 8 nm for PU-2 and less than 5 nm for PU-1 (Figure 2k,l). In smaller shells, the gaps are apparently wider. Consequently, weaker coupling of gold branches in small shells results in more prominent longitudinal plasmons. Overall one can conclude that, indeed, the structural variability of PUs can be translated into the fine tuning of the optical properties of the nanocapsules. It is also worthy to point out that the NIR absorption from the gold lace nanocapsules can be potentially convenient for optically triggered drug release and diagnostics. These interesting optical properties can also be exploited for SERS ultrasensitive analysis. Scattering spectra of a tradition SERS model compound, 1-nafthalenethiol, acquired on Au lace nanoshells and the comparison of the SERS intensity with that obtained from solid Au nanoparticles with no observable surface porosity or roughness of around 100 nm diameter (Figure S3), upon excitation with light from the visible to the NIR. Direct comparison of the intensities obtained in these cases indicates that Au lace shells give rise to larger enhancemet factors (EFs) upon illumination with the red laser line, consistent with a good coupling between the excitation beam and the localized surface plasmon resonance (LSPR) of the latter. However, by using NIR laser lines, 785 nm in particular, EFs dramatically increase to values larger than two orders of magnitude. This can be easily understood considering the close interbranch distances, which are in the order of 1–3 nm (Figure 1g), thus suitable to form highly active hot spots, while the excitation light is located close to the maximum of gold lace nanoshell absorption (Supplem. Mater. Fig. S2).

The actual performance of single particles as hotspots was demonstrated by isolation of single particles on a substrate and marking their position with a focusing ion beam. SEM, optical and SERS mapping of two different particles upon retention of benzenethiol (BT) from gas phase show that SERS signals can be only found at the positions where a lace colloid is located and, more importantly, a single particle is sufficient for the generation of an intense SERS signal (Fig. 4).

Considering the amphiphilic structure of PU globule, gold shells with entrapped waterborne PU should have a hydrophobic core which can be potentially used as a drug carrier or exploited in SERS detection as a mechanical trap.11 Pyrene was used as a model to test both the possibility of drug delivery from the gold lace shells and their efficiency to retain non common analytes for SERS detection. In fact, pyrene has only been detected using SERS by exploiting host guest interactions of calixarenes or aliphatic monolayers retained onto plasmonic particles.12 As expected, we observed that the luminescence of pyrene is strongly quenched after incubation with gold shells due to the incorporation of pyrene inside the nanoshells (Figure 6a, trace a) in complete analogy with Fabergé eggs. After equilibration, they were centrifuged washed and redispersed, retaining the previous molar concentration of nanoshells. The emission of pyrene can be observed again after pyrene escapes from gold

shells through nanoscale gaps and the intensity is increased with more pyrene diffusing out and plateaus after 30 h (Figure 6a, traces b–i). The recovery of luminescence indicates that the gaps in lace patterns of gold shells are sufficient for drug molecules to pass through. Complementary SERS experiments carried out on the same samples (Figure 6b), show that SERS signal of pyrene can be readily identified when retained onto the lace shells and lose intensity as the molecule is released. This is in full agreement with the SERS theory that indicates that a close proximity between particle and analyte is necessary to obtain an adequate signal and confirms both the trapping efficiency of the polymer shell and the potential for controlled release.

In summary, different sized branched gold lace shells with complex surface texture are obtained via a simple one-step reduction method using waterborne PUs as templates. The concentration of gold ions and the type of PUs are essential factors in determining the morphologies of gold nanostructures and their plasmonic properties which are found to be dominated by the size of the branches. The possibility of 3D carrier capacity of the gold lace nanoshells is demonstrated and will be under further investigation. The highly branched gold nanostructures were also demonstrated to be excellent substrates for further SERS investigations and the excellent biocompatibility of PU enables the facile biomedical applications. The use of SERS for real-time high resolution intracellular imaging should be considered in the future.

Supplementary Material

Refer to Web version on PubMed Central for supplementary material.

Acknowledgments

We acknowledge support of this research and Spanish MiCInn for a personal visiting grant to NAK. NAK also thanks support from NIH 5R01EB007350-02, 1R21CA121841-01A2, DARPA W31P4Q-08-C-0426NSF and NSF under grant ECS-0601345; EFRI-BSBA 0938019; CBET 0933384; and CBET 0932823. Any opinions, findings, and conclusions or recommendations expressed in this material are those of the authors and do not necessarily reflect the views of the National Science Foundation (NSF). The work is also partially supported by AFOSR MURI 444286-P061716. This material is based upon work partially supported by the Center for Solar and Thermal Energy Conversion, an Energy Frontier Research Center funded by the U.S. Department of Energy, Office of Science, Office of Basic Energy Sciences under Award Number #DE-SC0000957. The authors thank the University of Michigan's EMAL for its assistance with electron microscopy, and for the NSF grant #DMR-9871177 for funding for the JEOL 2010F analytical electron microscope used in this work. MY thanks Dr. Matthew Di Prima for English check-ups. RAA-P. acknowledges the RyC Program (MiCInn, Spain). Funding from the Spanish Ministerio de Ciencia e Innovacion/FEDER (MAT2007-62696 and MAT2008-05755) and the Xunta de Galicia (08TMT008314PR and 09TMT011314PR) grants is acknowledged. A. Benedetti (CACTI, U. Vigo) is thanked for the FIB marking and SEM imaging.

REFERENCES

1. a) Tao AR, Habas S, Yang PD. Small. 2008; 4:310–325. b) Sun YG, Xia YN. Science. 2002; 298:2176–2179. [PubMed: 12481134] c) Xiong YJ, Cai HG, Wiley BJ, Wang JG, Kim MJ, Xia YN. J. Am. Chem. Soc. 2007; 129:3665–3675. [PubMed: 17335211] d) Lu XM, Rycenga M, Skrabalak SE, Wiley B, Xia YN. Annu. Rev. Phys. Chem. 2009; 60:167–192. [PubMed: 18976140] e) Nie SM, Emery SR. Science. 1997; 275:1102–1106. [PubMed: 9027306] f) Sun YG, Xia YN. Analyst. 2003; 128:686–691. [PubMed: 12866889] g) Hirsch LR, Stafford RJ, Bankson JA, Sershen SR, Rivera B, Price RE, Hazle JD, Halas NJ, West JL. Proc. Natl. Acad. Sci. U.S.A. 2003; 100:13549–13554. [PubMed: 14597719] h) Lee JS, Han MS, Mirkin CA. Angew. Chem.-Int. Edit. 2007; 46:4093–4096.
2. a) Murphy CJ, San TK, Gole AM, Orendorff CJ, Gao JX, Gou L, Hunyadi SE, Li T. J. Phys. Chem. B. 2005; 109:13857–13870. [PubMed: 16852739] b) Murphy CJ, Sau TK, Gole A, Orendorff CJ. MRS Bull. 2005; 30:349–355.

3. a) Huo ZY, Tsung CK, Huang WY, Zhang XF, Yang PD. Nano Lett. 2008; 8:2041–2044. [PubMed: 18537294] b) Pastoriza-Santos I, Sanchez-Iglesias A, Rodriguez-Gonzalez B, Liz-Marzan LM. Small. 2009; 5:440–443. [PubMed: 19189327] c) Pastoriza-Santos I, Liz-Marzan LM. J. Mater. Chem. 2008; 18:1724–1737. d) Skrabalak SE, Chen JY, Sun YG, Lu XM, Au L, Cobley CM, Xia YN. Acc. Chem. Res. 2008; 41:1587–1595. [PubMed: 18570442] e) Jin RC, Cao YW, Mirkin CA, Kelly KL, Schatz GC, Zheng JG. Science. 2001; 294:1901–1903. [PubMed: 11729310]
4. a) Elghanian R, Storhoff JJ, Mucic RC, Letsinger RL, Mirkin CA. Science. 1997; 277:1078–1081. [PubMed: 9262471] b) Nam JM, Thaxton CS, Mirkin CA. Science. 2003; 301:1884–1886. [PubMed: 14512622] c) Rosi NL, Giljohann DA, Thaxton CS, Lytton-Jean AKR, Han MS, Mirkin CA. Science. 2006; 312:1027–1030. [PubMed: 16709779] d) Boisselier E, Astruc D. Chem. Soc. Rev. 2009; 38:1759–1782. [PubMed: 19587967] e) Boyer D, Tamarat P, Maali A, Lounis B, Orrit M. Science. 2002; 297:1160–1163. [PubMed: 12183624] f) Eghtedari M, Oraevsky A, Copland JA, Kotov NA, Conjusteau A, Motamedi M. Nano Lett. 2007; 7:1914–1918. [PubMed: 17570730] g) Ghosh P, Han G, De M, Kim CK, Rotello VM. Adv. Drug Deliv. Rev. 2008; 60:1307–1315. [PubMed: 18555555] h) Jan E, Byrne SJ, Cuddihy M, Davies AM, Volkov Y, Gun'ko YK, Kotov NA. ACS Nano. 2008; 2:928–938. [PubMed: 19206490] i) Kim K, Huang SW, Ashkenazi S, O'Donnell M, Agarwal A, Kotov NA, Denny MF, Kaplan MJ. Appl. Phys. Lett. 2007; 90 223901. j) Pissuwan D, Valenzuela SM, Cortie MB. Trends Biotechnol. 2006; 24:62–67. [PubMed: 16380179] k) Podsiadlo P, Sinani VA, Bahng JH, Kam NWS, Lee J, Kotov NA. Langmuir. 2008; 24:568–574. [PubMed: 18052300] l) Popovtzer R, Agrawal A, Kotov NA, Popovtzer A, Balter J, Carey TE, Kopelman R. Nano Lett. 2008; 8:4593–4596. [PubMed: 19367807] m) Sperling RA, Rivera gil P, Zhang F, Zanella M, Parak WJ. Chem. Soc. Rev. 2008; 37:1896–1908. [PubMed: 18762838] n) Yavuz MS, Cheng YY, Chen JY, Cobley CM, Zhang Q, Rycenga M, Xie JW, Kim C, Song KH, Schwartz AG, Wang LHV, Xia YN. Nat. Mater. 2009; 8:935–939. [PubMed: 19881498] o) Jin YD, Gao XH. J. Am. Chem. Soc. 2009; 131:17774–17776. [PubMed: 19928855] p) Qian XM, Peng XH, Ansari DO, Yin-Goen Q, Chen GZ, Shin DM, Yang L, Young AN, Wang MD, Nie SM. Nat. Biotechnol. 2008; 26:83–90. [PubMed: 18157119]
5. a) Bakr OM, Wunsch BH, Stellacci F. Chem. Mater. 2006; 18:3297–3301. b) Chen SH, Wang ZL, Ballato J, Foulger SH, Carroll DL. J. Am. Chem. Soc. 2003; 125:16186–16187. [PubMed: 14692749] c) Kumar PS, Pastoriza-Santos I, Rodriguez-Gonzalez B, Garcia de Abajo FJ, Liz-Marzan LM. Nanotechnology. 2008; 19 015606. d) Xie JP, Zhang QB, Lee JY, Wang DIC. ACS Nano. 2008; 2:2473–2480. [PubMed: 19206281] e) Averitt RD, Sarkar D, Halas NJ. Phys. Rev. Lett. 1997; 78:4217–4220.
6. a) Phadtare S, Kumar A, Vinod VP, Dash C, Palaskar DV, Rao M, Shukla PG, Sivaram S, Sastry M. Chem. Mater. 2003; 15:1944–1949. b) Hung HS, Hsu SH. Nanotechnology. 2007; 18 475101. c) Hsu SH, Chou CW. Polym. Degrad. Stabil. 2004; 85:675–680.
7. Zdrahala RJ, Zdrahala IJ. J Biomater. Appl. 1999; 14:67–90. [PubMed: 10405885]
8. a) Qian XM, Li J, Nie SM. J. Am. Chem. Soc. 2009; 131:7540–7541. [PubMed: 19453179] b) Alvarez-Puebla RA, Liz-Marzan LM. Small. 2010; 6:604–610. [PubMed: 20108237]
9. a) Yeh F, Hsiao BS, Sauer BB, Michel S, Siesler HW. Macromolecules. 2003; 36:1940–1954. b) Liff SM, Kumar N, McKinley GH. Nat. Mater. 2007; 6:76–83. [PubMed: 17173034] c) Dong AJ, Hou GL, Sun DX. J. Colloid Interface Sci. 2003; 266:276–281. [PubMed: 14527450] d) Nomula S, Cooper SL. J. Colloid Interface Sci. 1998; 205:331–339. [PubMed: 9735196] e) Cheong IW, Nomura M, Kim JH. Macromol. Chem. Phys. 2000; 201:2221–2227.
10. a) Hu M, Chen JY, Li ZY, Au L, Hartland GV, Li XD, Marquez M, Xia YN. Chem. Soc. Rev. 2006; 35:1084–1094. [PubMed: 17057837] b) Braun G, Pavel I, Morrill AR, Seferos DS, Bazan GC, Reich NO, Moskovits M. J Am. Chem. Soc. 2007; 129:7760–7761. [PubMed: 17539645]
11. a) Alvarez-Puebla RA, Contreras-Caceres R, Pastoriza-Santos I, Perez-Juste J, Liz-Marzan LM. Angew. Chem.-Int. Edit. 2009; 48:138–143. b) Abalde-Cela S, Ho S, Rodriguez-Gonzalez B, Correa-Duarte MA, Alvarez-Puebla RA, Liz-Marzan LM, Kotov NA. Angew. Chem.-Int. Edit. 2009; 48:5326–5329.
12. a) Jones CL, Bantz KC, Haynes CL. Anal. Bioanal. Chem. 2009; 394:303–311. [PubMed: 19263043] b) Guerrini L, Garcia-Ramos JV, Domingo C, Sanchez-Cortes S. Langmuir. 2006; 22:10924–10926. [PubMed: 17154566]

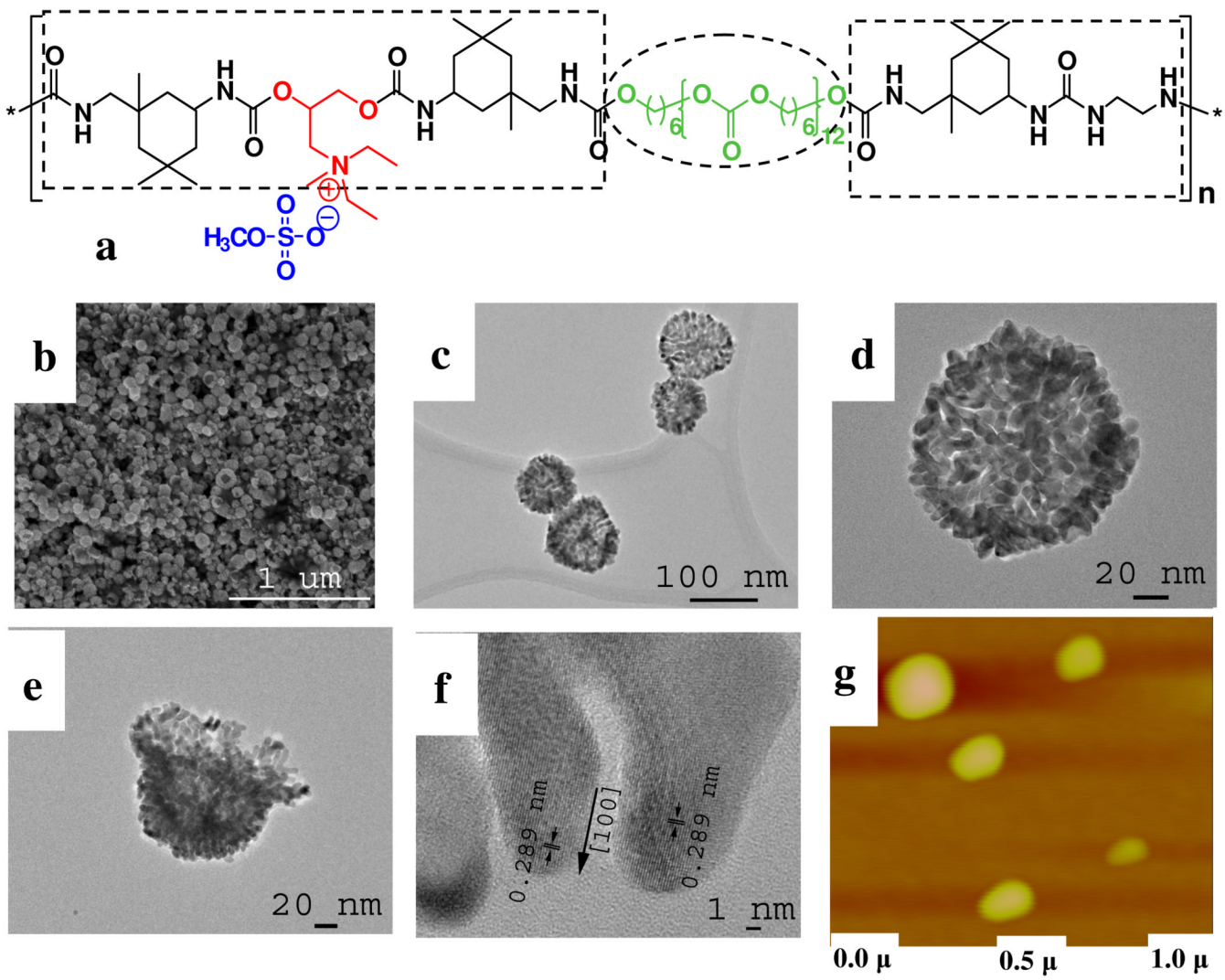

Figure 1.

(a) General molecular structure of PUs used in this study. The soft/hydrophobic part and hard/hydrophilic part are marked by dashed circles and rectangles, respectively. (b) SEM, (c–e) TEM and (f) HRTEM images of gold shells obtained by using PU-1 with 44 µM $HAuCl_4$. (g) Atomic force microscopy of the PU-1 globules dispersed in reaction media for synthesis of shells in b–e. vertical color scale 50 nm.

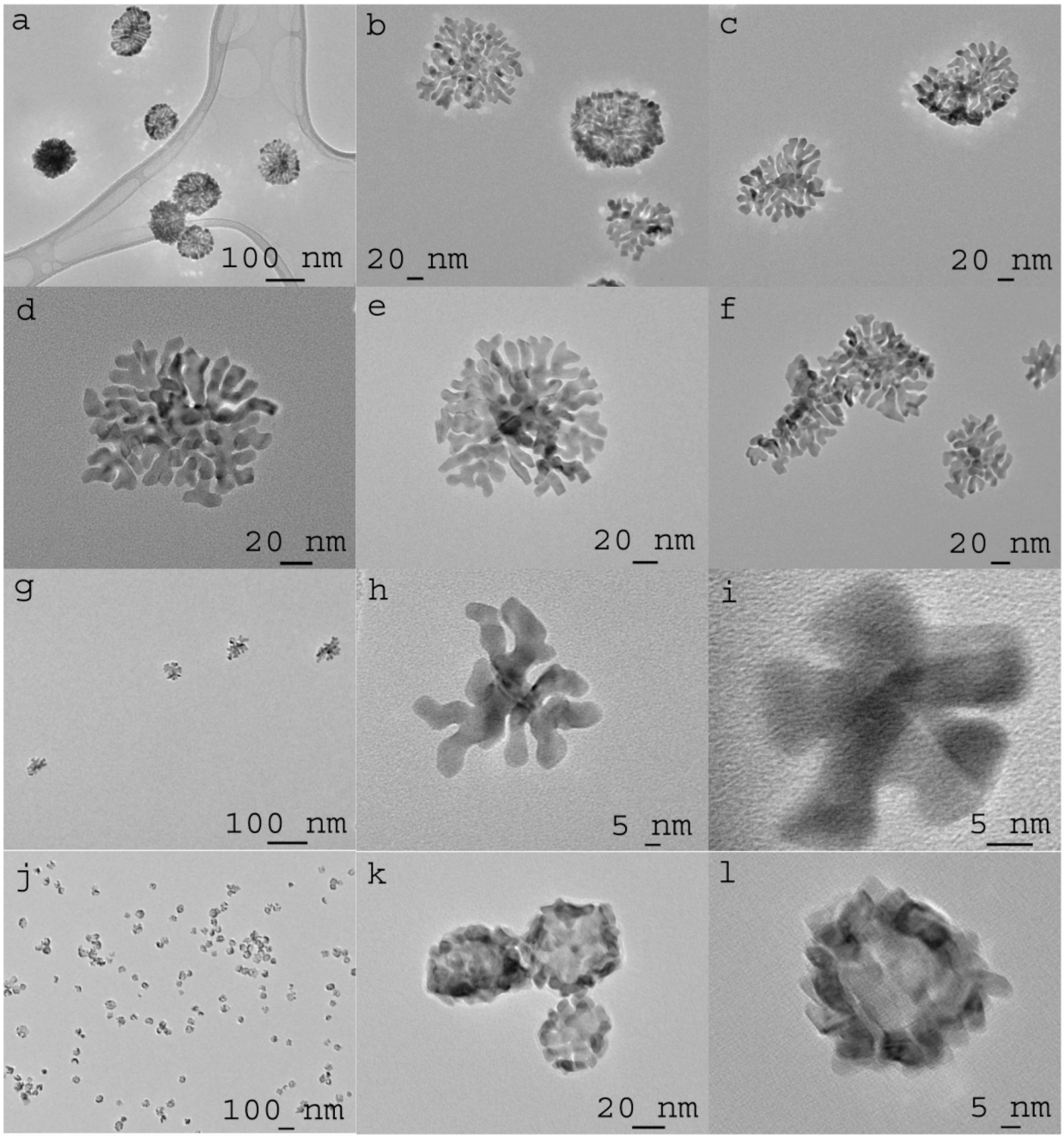

Figure 2.
TEM images of Au NPs obtained by using PU-1 with a–c) 36 μM, d–f) 28 μM and g–i) 20 μM $HAuCl_4$. j–l) TEM images of gold shells obtained with 44 μM $HAuCl_4$ using PU-2 with MW ≈ 77 kDa.

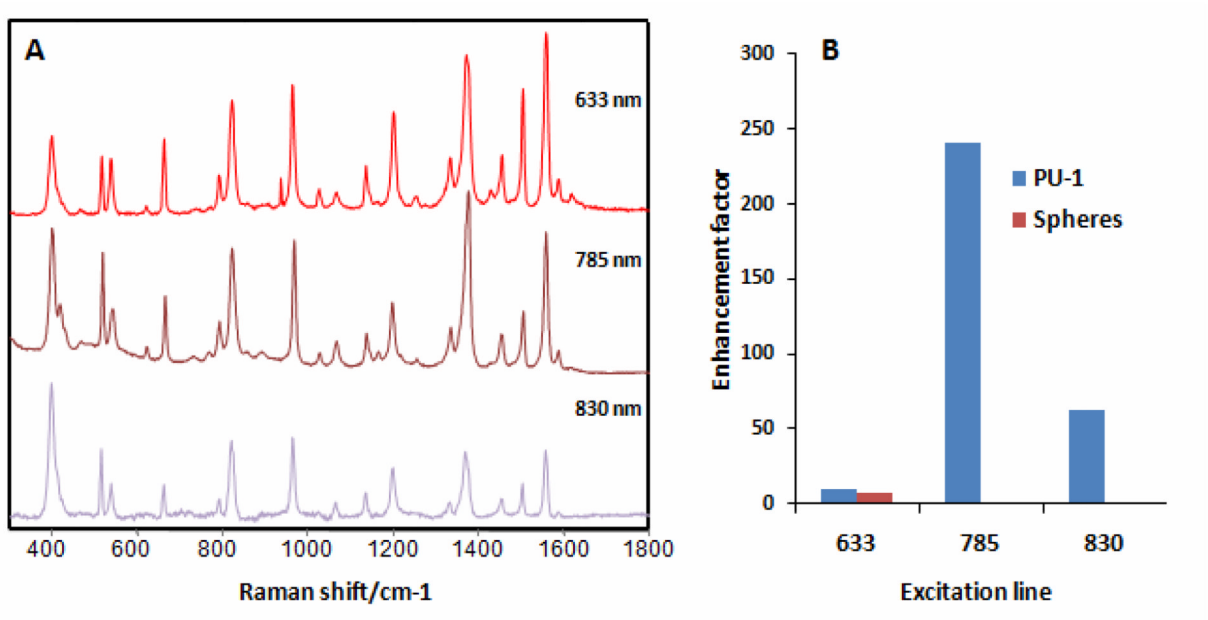

PU-2

Figure 3.

(a) SERS spectra of 1-naphthalenethiol upon excitation with 633, 785 and 830 nm laser lines. (b) Comparison of enhancement factors between gold lace shells and nanoscale solid spheres of similar size, as a function of the excitation line.

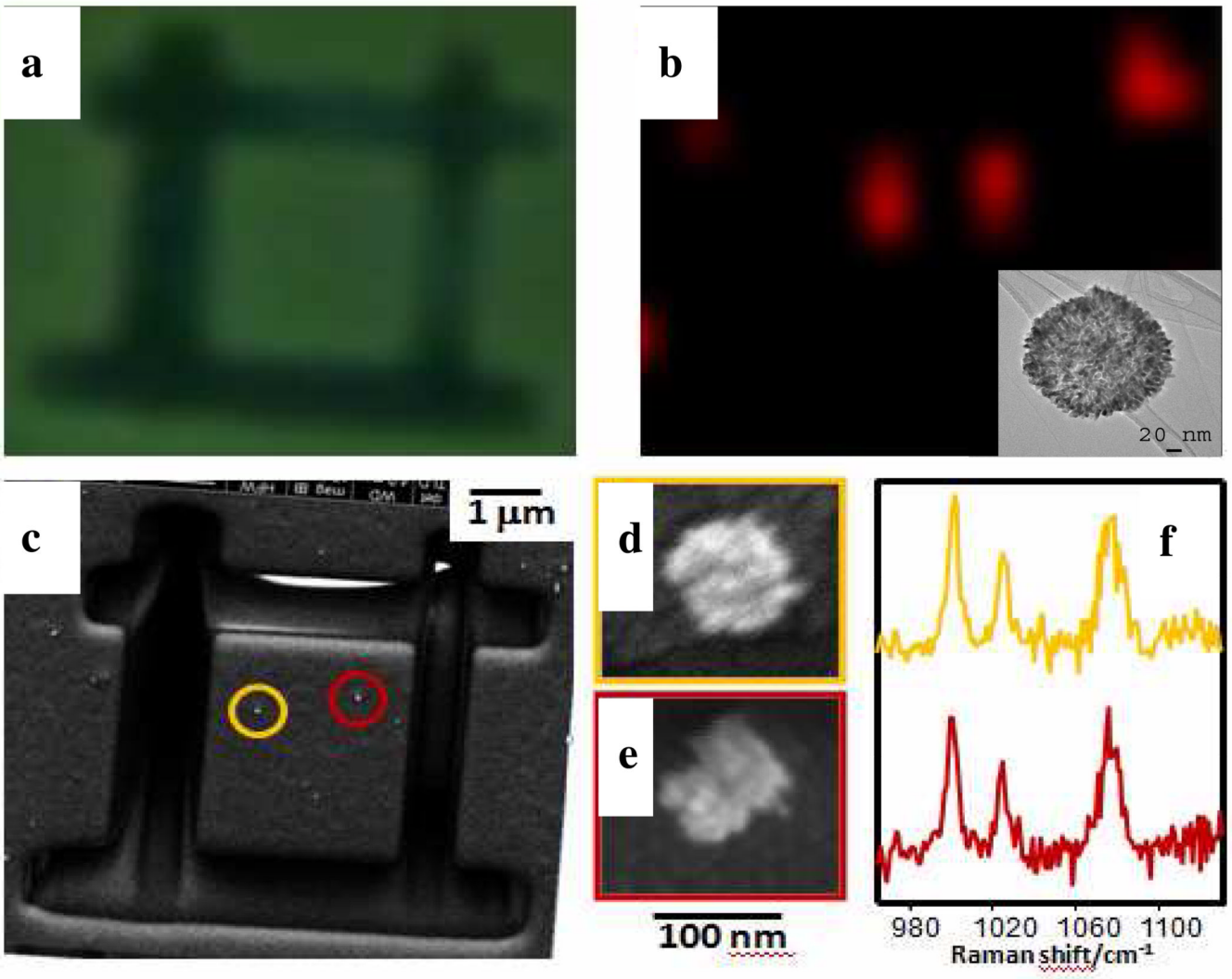

Figure 4.

Optical (a) and SERS (b) images of single lace NP. c–e) SEM images of the marked area; in the inset TEM image of the gold lace shells used in this experiment (c) and of two representative lace NPs (d,e). (f) SERS spectra corresponding to the laces shown in d (yellow) and e (red).

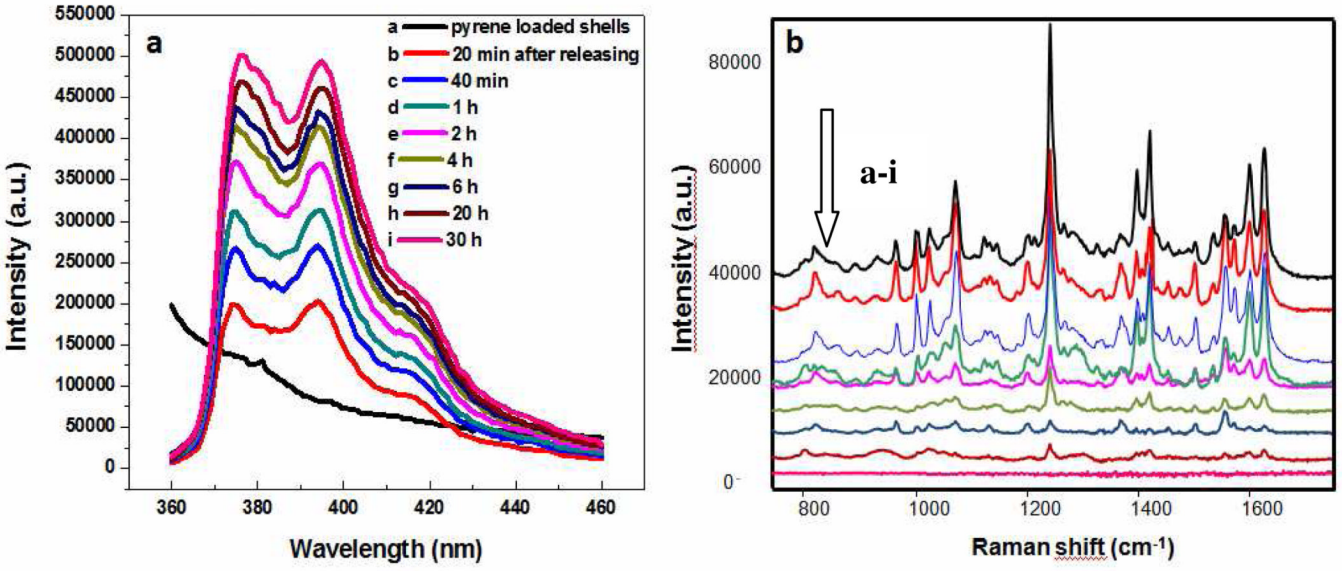

Figure 5.

Luminescence (a) and SERS (b) spectra of a) pyrene loaded gold shells, b–i) release medium after b) 20 min, c) 40 min, d) 1 h, e) 2 h, f) 4 h, g) 6 h, h) 20 h and i) 30 h. Luminescence spectra were recorded with excitation wavelength at 339 nm. The Raman scattering of water is subtracted from the spectra. SERS spectra were acquired upon excitation with 785 nm laser line with acquisition times of 10 s and 5 mW of power at the sample.